Supplementary Information

SI-1. Review of CSRE Catalysts

The past catalyst's development is shown in Figure S1, and illustrates how the focus for CSRE shifted from supported noble to non-noble metals. Both noble and non-noble catalysts were previously discussed by Deng et al. [1].

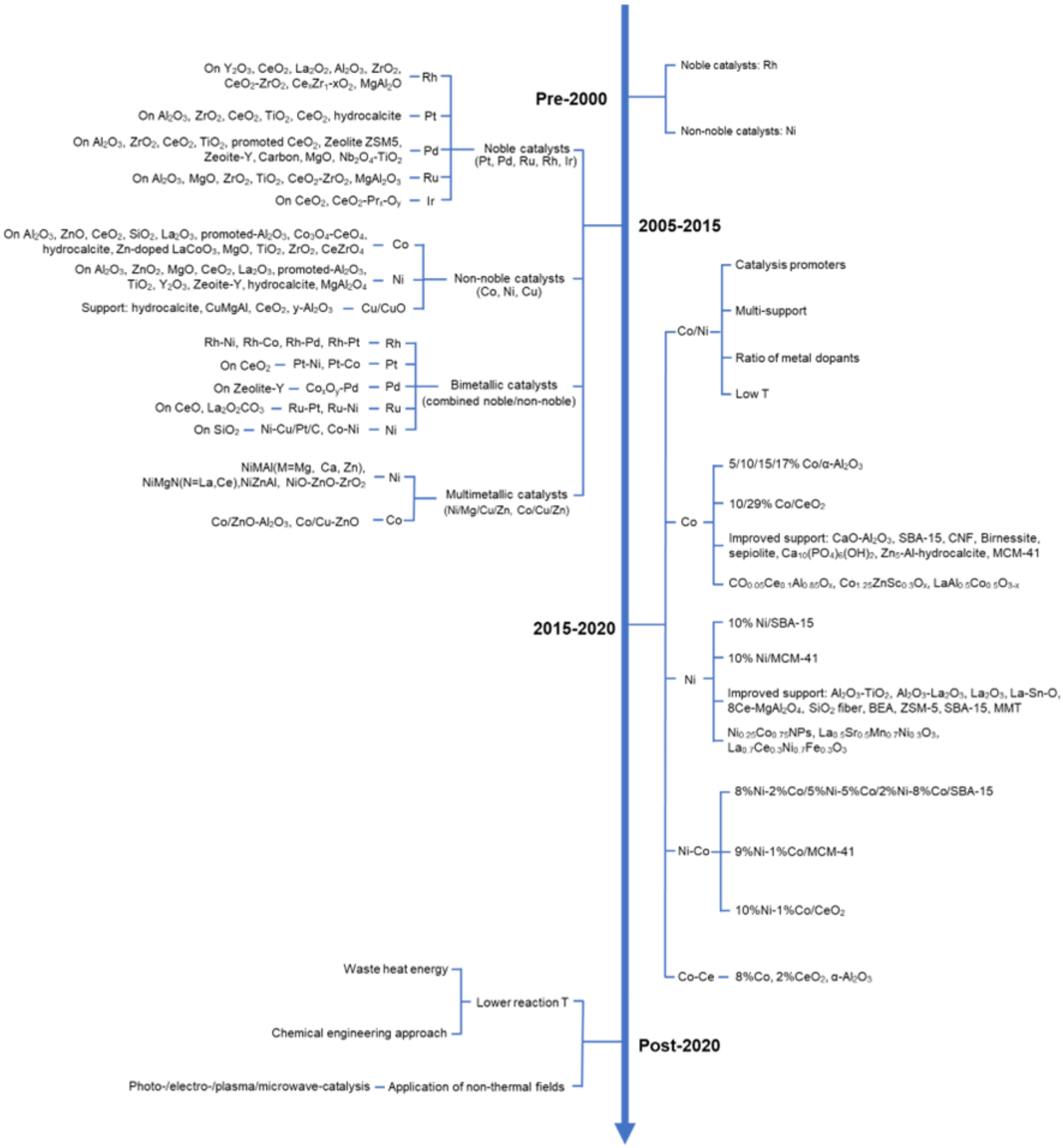

Figure S1. Literature Survey on CSRE.

The most recent catalyst developments, using mainly Co/Ni active species., are assessed in Table S1 and associated Figure S2a,b.

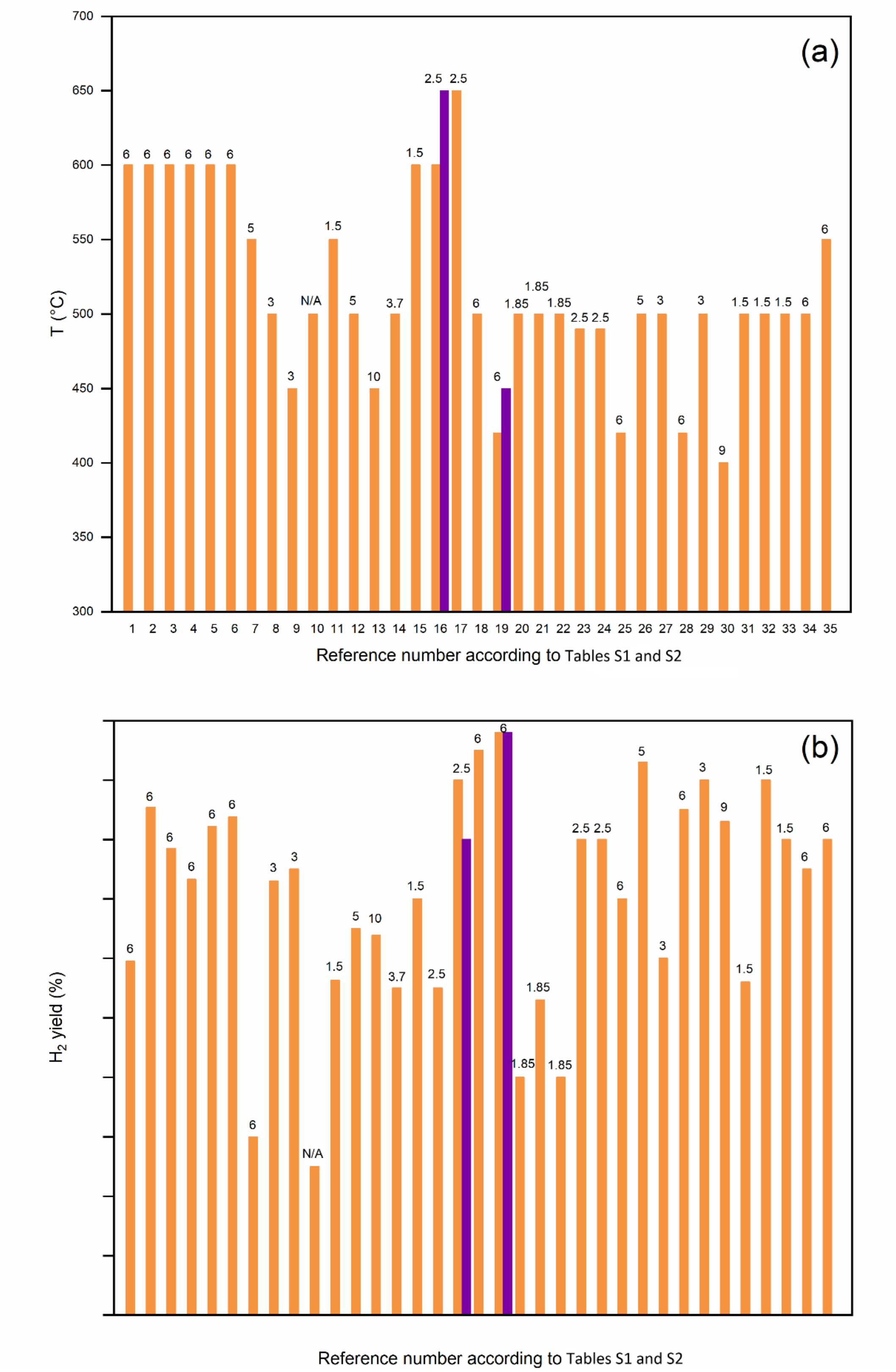

Figure S2. Key-process parameters of literature-cited CSRE (digits on top of the bars correspond to the molar S/E ratio) for (**a**) operating temperature and (**b**) H_2 yield. (orange bar refers to the first result of the reviewed reference; purple bar refers to the second result of the reviewed reference).

Table S1. Literature data (Before 2022).

No.	Catalyst	T (°C)	H_2 Yield (%)	Ref.
	Catalysts used in our research			
1	10Co/α-Al_2O_3	600	59.5	[1]
2	5Co-5Ni/α-Al_2O_3	600	85.4	[1]
3	5Co-5Cu/α-Al_2O_3	600	78.5	[1]
4	5Co-2Cu/α-Al_2O_3	600	73.3	[1]
5	3.3Co-3.3Ni-3.3Cu/α-Al_2O_3	600	82.2	[1]
6	2.5Fe-2.5Co-2.5Ni-2.5Cu/α-Al_2O_3	600	83.8	[1]
	Literature (Co-based)			
7	5Co/α-Al_2O_3	550	~30	[2]
8	17Co/α-Al_2O_3	500	~70	[3]
9	15Co/CaO -Al_2O_3	450	~70	[4]
10	5Co/Ca-hydroxyapatite	500	~25	[5]
11	5Co/Sr-hydroxyapatite	550	<60	[2]
12	$Co_{0.05}Ce_{0.1}Al_{0.85}O_x$	500	~65	[6]
13	10Co/CeO_2	450	<65	[7]
14	10Co/SBA-15	500	<55	[8]
15	10Co-7.1Ce/Sepiolite	600	<70	[9]
16	SiO_2@30($Co_{0.75}Mg_{0.25}O$)	600	~55	[10]
17	$LaAl_{0.5}Co_{0.5}O_{3-\delta}$	650	<90	[11]
18	29Co/CeO_2	500	~95	[12]
19	17Co/MnO_x	420	98	[13]
		450	98	[13]
	Literature (Ni/Co-based)			
20	10Ni/SBA-15	500	~40	[14]
21	8Ni-2Co/SBA-15	500	53	[14]
22	2Ni-8Co/SBA-15	500	~40	[8]
23	10Co/MCM-41	490	80	[15]
24	9Ni-1Co/MCM-41	490	80	[15]
25	10Ni/CeO_2	420	<70	[16]
26	10Co/CeO_2	500	93	[17]
27	10N-10Co/CeO_2	500	<60	[18]
28	2K/10Ni/CeO_2	420	85	[16]
29	$Ni_{0.25}Co_{0.75}$NPs	500	<90	[19]
30	5Cu-10Ni-10Co/hydrotalcite	400	83	[20]
31	10Ni/Al_2O_3-ZrO_2	500	56	[21]
32	10Ni/Al_2O_3-TiO_2	500	<90	[22]
33	8Ni-8Ca-1Au/CeO_2	500	80	[23]
34	10Ni/Zeolite	500	75	[24]
35	15Ni/Zeolite	550	<80	[25]

Table S2. Literature data (After 2022).

Catalyst	T (°C)	S/E	WHSV	H_2 Yield (%)	Ref.
5Ni/CZ-OP	550	3	GHSV = 10619 h^{-1}	~75	[26]
1%-NiCaOx/NaCl	650	3.4	GHSV = 12,160 h^{-1}	93	[27]
Ni/biochar	450	3	90.9 s^{-1}	<30	[28]
Ni-$CeLa_{0.2}$	600	4	55,920 mL EtOH solution/gcat·h	<40	[29]
Ni/Z-NS-IN	600	22	2286 h^{-1}	~60	[30]
10Ni-MBeta(DI)	600	5	0.5 mL EtOH solution/gcat·min	~75	[31]
PdNiSiO	600	3	GHSV = 48,500 h^{-1}	~60	[32]
30Ni5Cu/Al_2O_3-ZnO	600	4	N/A	63.6	[33]
Ni/La-Clay	500	6	N/A	<50	[34]
NiLaZimpr	550	6	W/F ratio = 144 g·h/g·mol	25	[35]
Ir-Fe/Al_2O_3	600	9.6	GHSV = 88,000 mL $g^{-1}\cdot h^{-1}$	~90	[36]
Ni/KIT-6	600	4	0.24 mL EtOH solution/gcat·min	~75	[37]
Ni-CaO-$CaZrO_3$	600	6	1.02 h^{-1}	>95	[38]
15Ni7.5Mg/HCa	650	6	GHSV = 10,000 h^{-1}	~90	[39]
Co/CeO_2	420	12	GHSV ≈ 1,286,000 mL/g·h	<20	[40]
Co/CeO_2-(M)	500	6	34,500 mL·$g^{-1}\cdot h^{-1}$	97	[41]
Co/ITQ-6	600	13	GHSV = 4700 h^{-1}	~70	[42]
15Ni–HCa	650	6	0.5 mL solution/gcat·min	86	[43]
Ni/ZIF-8	450	4	5.6 ml solution/gcat·h	68	[44]
$LaNi_{0.5}Co_{0.5}O_{3-\delta}$	600	5	N/A	~70	[45]

SI-2. Experimental Methods and Results of the Bio-Ethanol 2nd-Generation Process

SI-2.1. Production Process

Figure S3 illustrates the flowsheet of the test unit, with operating conditions and mass balance. Corn stover was used as feedstock.

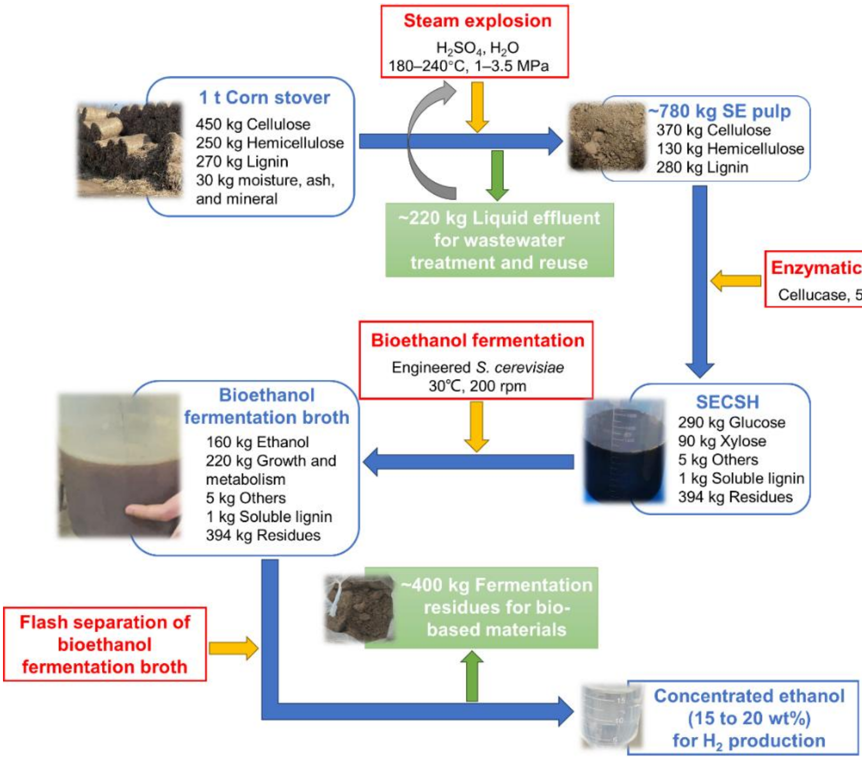

Figure S3. Ethanol fermentation from steam explosion (SE) corn stover hydrolysate (SECSH). "Others" in SECSH include weak acetic and formic acids, and furans such as furfural and 5-HMF.

Pretreatment of corn stover by steam explosion can effectively reduce the recalcitrant nature of the complex lignocellulosic matrix. Saccharification of SE pulp was performed for 96 h (50°C and 200 rpm) with 25 wt% of SE pulp dosage and 20 Filter Paper Unit (FPU)/g of cellulase loading via fed-batch enzymatic hydrolysis. A buffer of 0.05 M of H_3PO_4/KH_2PO_4 (pH 4.8) was applied [46]. Subsequently, ethanol fermentation was carried out, where an engineered strain, capable of utilizing the pentose fractions in the hydrolysate as carbon source, is applied. During the fermentation process, 10% (*v*/*v*) of *S. cerevisiae* was inoculated into SECSH at 30 °C and 200 rpm with optimum pH of 4.8. The mass balance of Figure 1 also indicates a residue of 394 kg. This biosolid residue can be applied to supply the heat requirements of the CSRE reactor.

SI-2.2. Experimental Set-Up and Results

The experimental layout was shown in Figure S4.

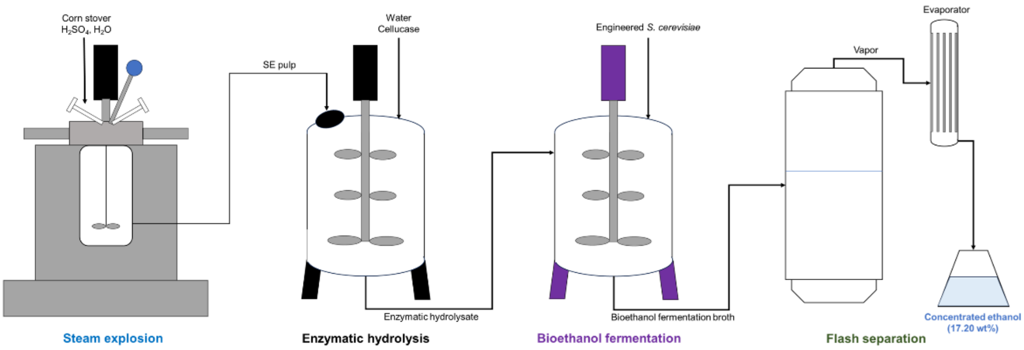

Figure S4. The experimental layout of second generation bioethanol refinery process

The composition of roughly evaporated bio-ethanol broth was shown in Table S3.

Table S3. Main components in roughly evaporated bio-EtOH broth

Components	Ethanol	Acetate	Acetaldehyde	Acetone
Content (wt%)	17.200	0.077	0.017	N.D.

N.D. Not detected.

The comparison between first- and second-generation bio-ethanol refinery process was shown in Table S4.

Table S4. The comparison between first- and second-generation bio-ethanol refinery process

	First-Generation	Second-Generation
Feedstocks	Food crops (e.g., corn, sugarcane, wheat).	Lignocellulosic biomass (e.g., agricultural and forestry waste, energy crops, etc.).
Environmental impacts	➢ Occupation of arable land, which may lead to food shortages and land degradation ➢ High greenhouse gas emissions	➢ Utilizing waste and reducing pollution from incineration and landfills ➢ Low greenhouse gas emissions
Main technical obstacles	Fluctuating feedstocks prices, land competition.	Pretreatment technology, enzymatic cost, ethanol-producing strain.
Pretreatment technology	No complex pretreatment required.	Pretreatment with high temperature and pressure, chemical or physical to increase hydrolysis efficiency.
Enzymatic hydrolysis	Simple or no enzymatic hydrolysis.	Demand for efficient enzyme systems to hydrolyze cellulose and hemicellulose.
Ethanol fermentation	➢ Carbon source is mainly glucose ➢ low inhibitors concentration ➢ high fermentation efficiency ➢ High ethanol concentration	➢ Carbon source is mainly glucose and xylose ➢ high inhibitors concentration ➢ low fermentation efficiency ➢ Moderate ethanol concentration
Economic viability	High economic viability and mature markets.	Medium economic feasibility.
Application	Commercialized for many years.	Demonstration line production, still in development and optimization phase.

In the second generation bioethanol refinery process, the fermentation broth is usually conveyed to a plate and frame filter to separate the solid residue. The filter cake obtained at the end of filtration can be further dried, pulverized, etc. for subsequent use as animal feed, wood-plastic materials, biomass energy generation, etc. [47–49].

Based on the mass balance of the bio-based process for bioethanol production from steam exploded corn stover, 780 kg of SE pulp was obtained from 1000 kg of corn stover after steam explosion. The biomass pretreatment method possessed various advantages such as energy savings and environmental friendliness [50,51]. In the saccharification stage, 290 kg of glucose and 90 kg of xylose can be recovered by enzymatic hydrolysis from the SE pulp. 1 kg of soluble lignins and 5 kg of inhibitors such as organic acids and furans were also contained in the recovered hydrolysate. These inhibitors would inhibit the growth and metabolism of *S. cerevisiae* [52,53]. Ultimately, in the fermentation stage, the detoxified enzymatic hydrolysate was inoculated with the xylose-assimilating *Saccharomyces cerevisiae* YL23-1, constructed by metabolic engineering and following adaptive laboratory evolution progresses [54]. Due to the effective utilization of xylose and high inhibitors' tolerance by the engineered strain YL23-1, the process generated 50.12 g/L of with a yield bio-ethanol of 0.42 g/g after batch inoculation for 96 h. Correspondingly, about 160 kg of bioethanol can be recovered from 1000 kg of dried corn stover. Ethanol in the fermentation broth can be recovered by flash separation to various ethanol-water concentration and used for H_2 production.

Reference

1. Deng, Y.; Li, S.; Appels, L.; Zhang, H.; Sweygers, N.; Baeyens, J.; Dewil, R. Steam reforming of ethanol by non-noble metal catalysts. *Renew. Sustain. Energy Rev.* **2023**, *175*, 113184. https://doi.org/10.1016/j.rser.2023.113184.
2. Ogo, S.; Maeda, S.; Sekine, Y. Coke Resistance of Sr-Hydroxyapatite Supported Co Catalyst for Ethanol Steam Reforming. *Chem. Lett.* **2017**, *46*, 729–732. https://doi.org/10.1246/cl.170072.
3. Riani, P.; Garbarino, G.; Canepa, F.; Guido, B. Cobalt nanoparticles mechanically deposited on α-Al_2O_3: A competitive catalyst for the production of hydrogen through ethanol steam reforming. *J. Chem. Technol. Biotechnol.* **2019**, *94*, 538–546. https://doi.org/10.1002/jctb.5800.

4. Han, S.J.; Song, J.W.; Yoo, J.; Park, S.; Kang, K.H.; Song, I.K. Sorption-enhanced hydrogen production by steam reforming of ethanol over mesoporous Co/$CaOAl_2O_3$ xerogel catalysts: Effect of Ca/Al molar ratio. *Int. J. Hydrogen Energy* **2017**, *42*, 5886–5898. https://doi.org/10.1016/j.ijhydene.2016.12.075.
5. Dobosz, J.; Małecka, M.; Zawadzki, M. Hydrogen generation via ethanol steam reforming over Co/HAp catalysts. *J. Energy Inst.* **2018**, *91*, 411–423. https://doi.org/10.1016/j.joei.2017.02.001.
6. de Lima, A.E.P.; de Oliveira, D.C. In situ XANES study of Cobalt in Co-Ce-Al catalyst applied to Steam Reforming of Ethanol reaction. *Catal. Today* **2017**, *283*, 104–109. https://doi.org/10.1016/j.cattod.2016.02.029.
7. Sohn, H.; Soykal, I.I.; Zhang, S.; Shan, J.; Tao, F.; Miller, J.T.; Ozkan, U.S. Effect of Cobalt on Reduction Characteristics of Ceria under Ethanol Steam Reforming Conditions: AP-XPS and XANES Studies. *J. Phys. Chem. C* **2016**, *120*, 14631–14642. https://doi.org/10.1021/acs.jpcc.6b02490.
8. Rodriguez-Gomez, A.; Holgado, J.P.; Caballero, A. Cobalt Carbide Identified as Catalytic Site for the Dehydrogenation of Ethanol to Acetaldehyde. *ACS Catal.* **2017**, *7*, 5243–5247. https://doi.org/10.1021/acscatal.7b01348.
9. Chen, M.;Wang, C.; Wang, Y.; Tang, Z.; Yang, Z.; Zhang, H.; Wang, J. Hydrogen production from ethanol steam reforming: Effect of Ce content on catalytic performance of Co/Sepiolite catalyst. *Fuel* **2019**, *247*, 344–355. https://doi.org/10.1016/j.fuel.2019.03.059.
10. Kim, K.M.; Kwak, B.S.; Im, Y.; Park, N.K.; Lee, T.J.; Lee, S.T.; Kang, M. Effective hydrogen production from ethanol steam reforming using CoMg co-doped $SiO_2@Co_{1-x}Mg_xO$ catalyst. *J. Ind. Eng. Chem.* **2017**, *51*, 140–152. https://doi.org/10.1016/j.jiec.2017.02.025.
11. Ohno, T.; Ochibe, S.; Wachi, H.; Hirai, H.; Arai, T.; Sakamoto, N.; Suzuki, H.; Matsuda, T. Preparation of metal catalyst component doped perovskite catalyst particle for steam reforming process by chemical solution deposition with partial reduction. *Adv. Powder Technol.* **2018**, *29*, 584–589. https://doi.org/10.1016/j.apt.2017.11.030.
12. Greluk, M.; Rotko, M.; Słowik, G.; Turczyniak-Surdacka, S. Hydrogen production by steam reforming of ethanol over Co/CeO_2 catalysts: Effect of cobalt content. *J. Energy Inst.* **2019**, *92*, 222–238. https://doi.org/10.1016/j.joei.2018.01.013.
13. Gac, W.; Greluk, M.; Słowik, G.; Turczyniak-Surdacka, S. Structural and surface changes of cobalt modified manganese oxide during activation and ethanol steam reforming reaction. *Appl. Surf. Sci.* **2018**, *440*, 1047–1062. https://doi.org/10.1016/j.apsusc.2018.01.242.
14. Rodriguez-Gomez, A.; Caballero, A. Bimetallic Ni-Co/SBA-15 catalysts for reforming of ethanol: How cobalt modifies the nickel metal phase and product distribution. *Mol. Catal.* **2018**, *449*, 122–130. https://doi.org/10.1016/j.mcat.2018.02.011.
15. Nejat, T.; Jalalinezhad, P.; Hormozi, F.; Bahrami, Z. Hydrogen production from steam reforming of ethanol over Ni-Co bimetallic catalysts and MCM-41 as support. *J. Taiwan Inst. Chem. Eng.* **2019**, *97*, 216–226. https://doi.org/10.1016/j.jtice.2019.01.025.
16. Słowik, G.; Greluk, M.; Rotko, M.; Machocki, A. Evolution of the structure of unpromoted and potassium-promoted ceria-supported nickel catalysts in the steam reforming of ethanol. *Appl. Catal. B: Environ.* **2018**, *221*, 490–509. https://doi.org/10.1016/j.apcatb.2017.09.052.
17. Sohn, H.; Celik, G.; Gunduz, S.; Dogu, D.; Zhang, S.; Shan, J.; Tao, F.F.; Ozkan, U.S. Oxygen Mobility in Pre-Reduced Nano- and Macro-Ceria with Co Loading: An AP-XPS, In-Situ DRIFTS and TPR Study. *Catal. Lett.* **2017**, *147*, 2863–2876. https://doi.org/10.1007/s10562-017-2176-4.
18. Pinton, N.; Vidal, M.V.; Signoretto, M.; Martínez-Arias, A.; Cortés Corberán, V. Ethanol steam reforming on nanostructured catalysts of Ni, Co and CeO_2: Influence of synthesis method on activity, deactivation and regenerability. *Catal. Today* **2017**, *296*, 135–143. https://doi.org/10.1016/j.cattod.2017.06.022.
19. Garbarino, G.; Cavattoni, T.; Riani, P.; Brescia, R.; Canepa, F.; Busca, G. On the Role of Support in Metallic Heterogeneous Catalysis: A Study of Unsupported Nickel–Cobalt Alloy Nanoparticles in Ethanol Steam Reforming. *Catal. Lett.* **2019**, *149*, 929–941. https://doi.org/10.1007/s10562-019-02688-9.
20. Shejale, A.D.; Yadav, G.D. Cu promoted Ni-Co/hydrotalcite catalyst for improved hydrogen production in comparison with several modified Ni-based catalysts via steam reforming of ethanol. *Int. J. Hydrogen Energy* **2017**, *42*, 11321–11332. https://doi.org/10.1016/j.ijhydene.2017.03.052.
21. Ángel-Soto, J.; Martínez-Rosales, M.; Ángel-Soto, P.; Zamorategui-Molina, A. Synthesis, characterization and catalytic application of Ni catalysts supported on alumina-zirconia mixed oxides. *Bull. Mater. Sci.* **2017**, *40*, 1309–1318. https://doi.org/10.1007/s12034-017-1493-y.
22. Gonçalves, A.A.S.; Faustino, P.B.; Assaf, J.M.; Jaroniec, M. One-Pot Synthesis of Mesoporous Ni-Ti-Al Ternary Oxides: Highly Active and Selective Catalysts for Steam Reforming of Ethanol. *ACS Appl. Mater. Interfaces* **2017**, *9*, 6079–6092. https://doi.org/10.1021/acsami.6b15507.
23. Menegazzo, F.; Pizzolitto, C.; Zanardo, D.; Signoretto, M.; Buysschaert, C.; Bény, G.; Di Michele, A. Hydrogen Production by Ethanol Steam Reforming on Ni-Based Catalysts: Effect of the Support and of CaO and Au Doping. *ChemistrySelect* **2017**, *2*, 9523–9531. https://doi.org/10.1002/slct.201702053.
24. Gac, W.; Greluk,M.; Słowik, G.; Millot, Y.; Valentin, L.; Dzwigaj, S. Effects of dealumination on the performance of

Ni-containing BEA catalysts in bioethanol steam reforming. *Appl. Catal. B Environ.* **2018**, *237*, 94–109. https://doi.org/10.1016/j.apcatb.2018.05.040.
25. Wang, S.; He, B.; Tian, R.; Sun, C.; Dai, R.; Li, X.; Wu, X.; An, X.; Xie, X. Ni-hierarchical Beta zeolite catalysts were applied to ethanol steam reforming: Effect of sol gel method on loading Ni and the role of hierarchical structure. *Mol. Catal.* **2018**, *453*, 64–73. https://doi.org/10.1016/j.mcat.2018.04.034.
26. Wang, M.; Kim, S.Y.; Jamsaz, A.; Pham-Ngoc, N.; Men, Y.; Jeong, D.H.; Shin, E.W. Metal-support interactions over Ni/CeO_2-ZrO_2 catalysts for ethanol steam reforming and their effects on the coke gasification. *Catal. Today* **2024**, *425*, 114341. https://doi.org/10.1016/j.cattod.2023.114341.
27. Hu, Y.; He, W.; Shen, Y. Hydrogen production from ethanol by steam reforming with recyclable $NiCaO_x$/NaCl catalysts. *Catal. Sci. Technol.* **2024**, *14*, 1062–1071. https://doi.org/10.1039/D3CY01701J.
28. Afolabi, A.T.F.; Kechagiopoulos, P.N.; Liu, Y.; Li, C.Z. Kinetic features of ethanol steam reforming and decomposition using a biochar-supported Ni catalyst. *Fuel Process. Technol.* **2021**, *212*, 106622. https://doi.org/10.1016/j.fuproc.2020.106622.
29. Xiao, Z.; Wu, C.; Wang, L.; Xu, J.; Zheng, Q.; Pan, L.; Zou, J.; Zhang, X.; Li, G. Boosting hydrogen production from steam reforming of ethanol on nickel by lanthanum doped ceria. *Appl. Catal. B Environ.* **2021**, *286*, 119884. https://doi.org/10.1016/j.apcatb.2021.119884.
30. Suriya, P.; Xu, S.; Ding, S.; Chansai, S.; Jiao, Y.; Hurd, J.; Lee, D.; Zhang, Y.; Hardacre, C.; Reubrocharoen, P.; et al. Ethanol steam reforming over Ni/ZSM-5 nanosheet for hydrogen production. *Chin. J. Chem. Eng.* **2024**, *67*, 247–256. https://doi.org/10.1016/j.cjche.2023.12.006.
31. Wang, S.; He, B.; Wang, Y.; Wu, X.; Duan, H.; Di, J.; Yu, Z.; Liu, Y.; Xin, Z.; Jia, L.; et al. Hydrogen production from the steam reforming of bioethanol over novel supported Ca/Ni-hierarchical Beta zeolite catalysts. *Int. J. Hydrogen Energy* **2021**, *46*, 36245–36256. https://doi.org/10.1016/j.ijhydene.2021.08.170.
32. Chagas, C.A.; Manfro, R.L.; Toniolo, F.S. Production of Hydrogen by Steam Reforming of Ethanol over Pd-Promoted Ni/SiO2 Catalyst. *Catal. Lett.* **2020**, *150*, 3424–3436. https://doi.org/10.1007/s10562-020-03257-1.
33. Liu, Q.; Zhou, H.; Jia, Z. Hydrogen Production by Ethanol Reforming on Supported Ni-Cu Catalysts. *ACS Omega* **2022**, *7*, 4577–4584. https://doi.org/10.1021/acsomega.1c06579.
34. Boudadi, K.; Bellifa, A.; Márquez-Álvarez, C.; Corberán, V.C. Nickel catalysts promoted with lanthanum for ethanol steam reforming: Influence of support and treatment on activity. *Appl. Catal. A Gen.* **2021**, *619*, 118141. https://doi.org/10.1016/j.apcata.2021.118141.
35. Pizzolitto, C.; Menegazzo, F.; Ghedini, E.; Innocenti, G.; Michele, A.D.; Mattarelli, M.; Cruciani, G.; Cavani, F.; Signoretto, M. Ethanol Steam Reforming on Lanthanum Ni-ZrO2 Catalysts. *ACS Sustain. Chem. Eng.* **2020**, *8*, 10756–10766. https://doi.org/10.1021/acssuschemeng.0c02373.
36. Choong, C.K.S.; Du, Y.; Poh, C.K.; Ong, S.W.D.; Chen, L.; Borgna, A. Structural understanding of IrFe catalyst for renewable hydrogen production from ethanol steam reforming. *Appl. Catal. B Environ. Energy* **2024**, *345*, 123630. https://doi.org/10.1016/j.apcatb.2023.123630.
37. Bkangmo Kontchouo, F.M.; Shao, Y.; Zhang, S.; Gholizadeh, M.; Hu, X. Steam reforming of ethanol, acetaldehyde, acetone and acetic acid: Understanding the reaction intermediates and nature of coke. *Chem. Eng. Sci.* **2023**, *265*, 118257. https://doi.org/10.1016/j.ces.2022.118257.
38. Wang, Y.; Zhou, Hui.; Yao, D.; Olguin, G.; Ding, H.; Qu, B.; Xie, W.; Fu, Z.; Guo, Y.; Wang, X.; Li, A.; et al. Ni-CaO-$CaZrO_3$ bi-functional materials for high purity hydrogen production via sorption enhanced steam reforming of ethanol. *J. Clean. Prod.* **2024**, *446*, 141397. https://doi.org/10.1016/j.jclepro.2024.141397.
39. Liu, H.; Ding, R.; Zhang, Y.; Li, H.; Li, S. Magnesium promoted hydrocalumite derived nickel catalysts for ethanol steam reforming. *Int. J. Hydrogen Energy* **2023**, *48*, 13804–13813. https://doi.org/10.1016/j.ijhydene.2022.12.295.
40. Greluk, M.; Gac, W.; Rotko, M.; Słowik, G.; Turczyniak-Surdacka, S. Co/CeO_2 and Ni/CeO_2 catalysts for ethanol steam reforming: Effect of the cobalt/nickel dispersion on catalysts properties. *J. Catal.* **2021**, *393*, 159–178. https://doi.org/10.1016/j.jcat.2020.11.009.
41. Li, R.; Liu, C.; Li, L.; Xu, J.; Ma, J.; Ni, J.; Yan, J.; Han, J.; Pan, Y.; Liu, Y.; et al. Regulating cobalt chemical state by CeO_2 facets preferred exposure for improved ethanol steam reforming. *Fuel* **2023**, *336*, 126758. https://doi.org/10.1016/j.fuel.2022.126758.
42. Da Costa-Serra, J.F.; Miralles-Martínez, A.; García-Muñoz, B.; Maestro-Cuadrado, S.; Chica, A. Ni and Co-based catalysts supported on ITQ-6 zeolite for hydrogen production by steam reforming of ethanol. *Int. J. Hydrogen Energy* **2023**, *48*, 26518–26525. https://doi.org/10.1016/j.ijhydene.2022.11.128.
43. Liu, H.; Li, H.; Li, S. Ni-hydrocalumite derived catalysts for ethanol steam reforming on hydrogen production. *Int. J. Hydrogen Energy* **2022**, *47*, 24610–24618. https://doi.org/10.1016/j.ijhydene.2021.07.141.
44. Razavian, M.; Fatemi, S.; Malek mohammadi, M.; Nouralishahi, A. Nickel supported ZIF-8.PEG modified catalyst: A designed active catalyst with high H_2 productivity in steam reforming of ethanol at moderate temperature. *J. Environ. Chem. Eng.* **2021**, *9*, 105531. https://doi.org/10.1016/j.jece.2021.105531.

45. Shen, Q.; Jiang, Y.; Li, S.; Yang, G.; Zhang, H.; Zhang, Z.; Pan, X. Hydrogen production by ethanol steam reforming over Ni-doped $LaNixCo_{1-x}O_{3-\delta}$ perovskites prepared by EDTA-citric acid sol–gel method. *J. Sol-Gel Sci. Technol.* **2021**, *99*, 420–429. https://doi.org/10.1007/s10971-021-05588-w.
46. Zhang, C.; Wen, H.; Chen, C.; Cai, D.; Fu, C.; Li, P.; Qin, P.; Tan, T. Simultaneous saccharification and juice co-fermentation for high-titer ethanol production using sweet sorghum stalk. *Renewable Energy* **2019**, *134*, 44–53. https://doi.org/10.1016/j.renene.2018.11.005.
47. Hosseinaei, O.; Wang, S.; Enayati, A.A.; Rials, T.G. Effects of hemicellulose extraction on properties of wood flour and wood–plastic composites. *Compos. Part A* **2012**, *43*, 686–694. https://doi.org/10.1016/j.compositesa.2012.01.007.
48. Bizzo, W.A.; Lenco, P.C.; Carvalho, D.J.; Veiga, J.P.S. The generation of residual biomass during the production of bio-ethanol from sugarcane, its characterization and its use in energy production. *Renew. Sustain. Energy Rev.* **2014**, *29*, 589–603. https://doi.org/10.1016/j.rser.2013.08.056.
49. Chiesa, S.; Gnansounou, E. Protein extraction from biomass in a bioethanol refinery—Possible dietary applications: Use as animal feed and potential extension to human consumption. *Bioresourse Technol.* **2011**, *102*, 427–436. https://doi.org/10.1016/j.biortech.2010.07.125.
50. Wu, Y.; Wen, J.; Su, C.; Jiang, C.; Zhang, C.; Wang, Y.; Jiang, Y.; Ren, W.; Qin, P.; Cai, D. Inhibitions of microbial fermentation by residual reductive lignin oil: Concerns on the bioconversion of reductive catalytic fractionated carbohydrate pulp. *Chem. Eng. J.* **2023**, *452*, 139267. https://doi.org/10.1016/j.cej.2022.139267.
51. Su, C.; Zhang, C.; Wu, Y.; Zhu, Q.; Wen, J.; Wang, Y.; Zhao, J.; Liu, Y.; Qin, P.; Cai, D. Combination of pH adjusting and intermittent feeding can improve fermentative acetone-butanol-ethanol (ABE) production from steam exploded corn stover. *Renew. Energy* **2022**, *200*, 592–600. https://doi.org/10.1016/j.renene.2022.10.008.
52. Yu, Y.; Wu, J.; Ren, X.; Lau, A.; Rezaei, H.; Takada, M.; Bi, X.; Sokhansanj, S. Steam explosion of lignocellulosic biomass for multiple advanced bioenergy processes: A review. *Renew. Sustain. Energy Rev.* **2022**, *154*, 111871. https://doi.org/10.1016/j.rser.2021.111871.
53. Li, B.; Liu, N.; Zhao, X. Response mechanisms of Saccharomyces cerevisiae to the stress factors present in lignocellulose hydrolysate and strategies for constructing robust strains. *Biotechnol. Biofuels Bioprod.* **2022**, *15*, 28. https://doi.org/10.1186/s13068-022-02127-9.
54. Wu, Y.; Su, C.; Zhang, G.; Liao, Z.; Wen, J.; Wang, Y.; Jiang, Y.; Zhang, C.; Cai, D. High-Titer Bioethanol Production from Steam-Exploded Corn Stover Using an Engineering Saccharomyces cerevisiae Strain with High Inhibitor Tolerance. *Fermentation* **2023**, *9*, 906. https://doi.org/10.3390/fermentation9100906.